Eur Biophys J (2010) 39:1581–1588
DOI 10.1007/s00249-010-0615-x

ORIGINAL PAPER

Deglycosylated milin unfolds via inactive monomeric intermediates

Subhash Chandra Yadav · N. K. Prasanna Kumari · Medicherla V. Jagannadham

Received: 8 March 2010 / Revised: 23 May 2010 / Accepted: 26 May 2010 / Published online: 13 June 2010

Abstract The effect of deglycosylation on the physiological and functional organization of milin was studied under different denaturizing conditions. Trifluoromethanesulfonic acid mediated deglycosylation resulted in insoluble milin, which was found to be soluble only in 1.5 M GuHCl with native-like folded structure. Kinetic stability, proteolytic activity, and dimeric association were lost in deglycosylated milin. Urea-induced unfolding revealed two inactive, highly stable equilibrium intermediates at pH 7.0 and pH 2.0. These intermediates were stable between 5.5–6.5 and 5.0–6.0 M total chaotropes (urea + 1.5 M GuHCl) at pH 7.0 and pH 2.0, respectively. GuHCl-induced unfolding was cooperative and noncoincidental with a broad transition range (2.0–5.0 M) at pH 7.0 and pH 2.0. Equilibrium unfolding of deglycosylated milin by urea and GuHCl substantiates the involvement of various inactive monomeric intermediates. This study provides a way to understand the role of glycosylation in the unfolding mechanism, stability, and functional activity of the serine protease milin.

Keywords Deglycosylation · Serine protease · Milin · Trifluoromethanesulfonic acid · Folding · Monomeric intermediate

S. C. Yadav · N. K. Prasanna Kumari · M. V. Jagannadham (✉)
Molecular Biology Unit, Institute of Medical Sciences, Banaras Hindu University, Varanasi 221005, UP, India
e-mail: jvm@bhu.ac.in

S. C. Yadav (✉)
Nanobiology Lab, Biotechnology Division, Institute of Himalayan Bioresource Technology (CSIR), Palampur 176061, HP, India
e-mail: subhash@ihbt.res.in

Abbreviations

GuHCl	Guanidine hydrochloride
TFMS	Trifluoromethanesulfonic acid
UV	Ultraviolet
CD	Circular dichroism
ANS	1-Anilino-8-naphthalene sulfonic acid

Introduction

Glycosylation of proteins helps in correct folding, stability, function, solubility, and secretion (Daniels et al. 2003; Petrescu et al. 2000). The molecular composition and peptide backbone location of the glycan moieties have a critical and unique conformational effect on protein structure (Gagneux and Varki 1999; Varki 1993). This glycosylation is crucial to provide extra stability and high aqueous solubility to glycoproteins. These carbohydrate moieties of glycoproteins are involved in cell–cell communication, immune response, cell adhesion, intracellular targeting, protease resistance, and many other processes (Petrescu et al. 2000; Reuter and Gabius 1999; Varki 1993). Among the various types of glycosylation, *N*-linked glycosylation is common in most plant serine proteases. This type of glycosylation takes place cotranslationally during protein biosynthesis in the ribosome and has a tendency to affect the protein folding pathway (Imperiali and O'Connor 1999; O'Connor and Imperiali 1996); for example, *N*-acetamido group of glycan induces a well-defined type I β-turn in the peptide backbone (O'Conner and Imperiali 1998), providing a unique conformational effect on the interglycosidic and glycopeptides linkage. This results in a precise conformation of the peptide

backbone (Bosques et al. 2004). In addition, the glycan moiety attached to a newly synthesized protein influences the folding sequence. This leads to the formation of organized tertiary structure. Furthermore, oligosaccharides cover functionally important area (active site) of the protein (Petrescu et al. 2000).

Detailed empirical characterization of posttranslational modification of proteins is useful to understand the role of glycosylation in various physiological pathways (Kuster et al. 2001). Investigation of many cellular processes and their regulation are best studied at the protein level due to posttranslational modification such as glycosylation, phosphorylation, etc. Protein glycosylation is a common means to target proteins, regulating their activity and mediating signal transduction. These are mainly influenced by specific species, tissue, and cell types. Therefore, it is highly desirable to study naturally expressed glycoprotein rather than recombinant protein for the evaluation of protein structural stability and folding behavior. Glycan moieties are able to modify the physiological and biophysical properties of proteins by altering surface charges, stability, and protease susceptibility (Kuster et al. 2001). Glycosylation can induce bulky hydrophilic groups which provide structural stability during the folding process (Bernard et al. 1983). Understanding the role of complete deglycosylation in protein folding is important. Enzymatic deglycosylation is not suitable for unfolding studies of kinetically stable proteins because it acts prior to complete denaturation of glycoproteins (Hirsch et al. 2004). Thus, TFMS deglycosylation is preferred to avoid protein denaturation during deglycosylation for unfolding studies of glycoproteins (Edge 2003). We have deglycosylated milin chemically by using TFMS to study unfolding of this protein. The role of glycosylation in the folding–unfolding behavior of glycoproteins is of interest in current research to aid understanding of various physiological and pathological processes (Shental-Bechor and Levy 2008).

The goal of the present study is to investigate the effect of glycosylation on the unfolding behavior of the serine protease milin. The unfolding mechanism of native milin shows multiple dimeric intermediates, some of which are partially active (Yadav et al. 2010). The carbohydrate moiety seems to be part of the functional architecture of milin and to be linked by *N*-glycosidic linkage (Lynn and Clevette-Radford 1988; Wujek et al. 2004). However, the loss of proteolytic activity of deglycosylated milin suggests the impact of glycosylation on the structure and function of glycoproteins. Herein, we report the folding behavior and characterization of intermediates during unfolding of deglycosylated milin.

Materials and methods

Materials

Latex of *Euphorbia milii* was used to purify milin as previously described (Yadav et al. 2006). Protein concentration was determined using an extinction coefficient of $\varepsilon_{280}^{1\%} = 11.10$ (Yadav et al. 2009) as well as by Bradford assay. Urea and GuHCl were procured from Sigma Chemical Company, USA. ANS was from Aldrich, USA. All other chemicals were of highest commercially available purity. Concentration of urea and GuHCl were determined using refractometry (Pace et al. 1996). Enzyme samples were prepared in Millipore water and filtered through 0.45 μm filters.

Methods

Deglycosylation of milin by TFMS

Milin was chemically deglycosylated by using trifluoromethanesulfonic acid (TFMS) (Edge 2003). Lyophilized milin (1 mg) was incubated at −20°C with 150 μl prechilled (−20°C) working TFMS solution (containing anisole, 1:1 v/v) for 30 min. The reaction was neutralized by adding 6% prechilled pyridine. The pyridine solution was diluted using 1:1 v/v methanol:water solution. The reaction solution was desalted by dialysis. Precipitated deglycosylated milin was solubilized in 1.5 M GuHCl at neutral pH and used for further unfolding studies. For sodium dodecyl sulfate polyacrylamide gel electrophoresis (SDS–PAGE), precipitated deglycosylated milin was heated with sample buffer for 15 min at 95°C and loaded onto 15% polyacrylamide gels (Yadav et al. 2009).

Activity

The hydrolyzing activity of the protease was determined using denatured natural substrates such as casein and hemoglobin as previously described (Yadav et al. 2006). Active enzyme was taken as indicating functional native protein, while specific activity as reported before was taken as indicating protein purity. Deglycosylated milin solubilized in 1.5 M GuHCl, as prepared above, was also assayed against casein. Native, glycosylated enzyme in 1.5 M GuHCl was used as a reference for such measurements.

Circular dichroism, fluorescence, and absorbance

Circular dichroism (CD) spectra of milin under various conditions were recorded using a JASCO 500A spectropolarimeter, precalibrated using 0.1% d-10-camphorsulfonic

acid solution (Cassim and Yang 1969). This method was briefly described in our earlier publication (Yadav et al. 2009).

Secondary structures in the protein were monitored using far-ultraviolet (far-UV) CD spectra in the wavelength range 200–260 nm, with protein concentration of 0.1 mg/ml in 1.0-mm-path-length cuvette.

Results are expressed as mean residue ellipticity $[\theta]_{MRW}$ using the equation

$$[\theta]_{MRW} = \theta_{obs} \times MRW/10 \cdot c \cdot l,$$

where θ_{obs}, c, and l are the observed ellipticity in degrees, protein concentration in mg/ml, and the path length of the light in cm, respectively. Mean weight of amino acid residues (MRW) was taken as 110. The secondary structural content (α-helix, β-sheets) of the proteins was calculated using software provided by JASCO.

ANS binding

The extent of exposure of hydrophobic surfaces in the enzyme was determined by its ability to bind to the fluorescent dye ANS (Stryer 1965). The details of this method were described elsewhere (Yadav et al. 2009).

Chemical unfolding of milin

Unfolding of milin was monitored by equilibrating protein samples at given denaturant (GuHCl and urea) concentration for 24 h at room temperature before optical or enzymatic measurements (Yadav et al. 2009).

The fraction of unfolded protein (F) at any denaturant concentration was calculated using the equation

$$F = (F_n - F_{obs})/(F_n - F_u),$$

where, F_n and F_u represent the value of F (factors) characteristic of completely folded (native) and completely unfolded (denatured) states, respectively. F_{obs} represents the value of F (factor) at a particular condition.

Results

The effect of different chaotropes on the conformation, structure–function relationship, and folding of deglycosylated milin was investigated under equilibrium conditions at physiological temperature by employing far-UV circular dichroism, tryptophan fluorescence, UV absorbance, and ANS binding.

Deglycosylation of milin reduces solubility

Milin was chemically deglycosylated to evaluate the role of glycosylation in protein folding, stability, and solubility. A single monomeric band of deglycosylated milin appeared at 30 kDa in SDS–PAGE (Yadav et al. 2009). Deglycosylated milin was insoluble and precipitated. TFMS deglycosylation preferably resulted in peptide cleavage (acid hydrolysis) of acid-labile peptide bonds such as DP, DH, etc. However, SDS-PAGE revealed no such peptide cleavage after deglycosylation of milin (Yadav et al. 2009). It was found to be soluble only in 1.5 M GuHCl with its full structural entities. This minimum concentration of GuHCl (1.5 M GuHCl) for solubility of deglycosylated milin was therefore present in all further denaturation experiments. This condition was assumed to correspond to native deglycosylated milin.

Deglycosylation of milin leads to proteolytic inactivation

Deglycosylated milin was proteolytically inactive. One reason could be the presence of 1.5 M GuHCl, but it should be noted that dimeric glycosylated native milin retains 80% of its proteolytic activity in 1.5 M GuHCl (Yadav et al. 2006, 2010). This was taken as evidence of protection of active site by glycosylation at the surface of milin. Generally, glycosylation does not have any role in active sites and activity, but it provides protection to active site tetrad of serine protease milin.

Spectroscopic characterization of deglycosylated milin

Since deglycosylated milin lost its functional activity, we investigated its conformational behavior under denaturizing conditions at pH 7.0 and 2.0. The structural organization of deglycosylated milin was distorted in comparison with native glycosylated milin, as shown by loss of activity, insolubility, and loss of dimeric association. Far-UV CD of deglycosylated milin (1.5 M GuHCl) was centered at 217 nm with a small shoulder at 222 nm similar to α/β class of glycosylated milin in 1.5 M GuHCl (Fig. 1a) (Yadav et al. 2009). The molar ellipticity at 217 nm was $-9.0 \pm 0.20 \times 10^3$ deg cm^2/dmol (Fig. 1a). The magnitude of the molar residual ellipticity was similar to that of native milin in 1.5 M GuHCl (Yadav et al. 2009). The far-UV CD spectrum of enzyme was completely lost in 6 M GuHCl at pH 7.0 (Fig. 1a). However, 6 M GuHCl eliminated only 40% of the far-UV CD signal of glycosylated milin at neutral pH.

Intrinsic fluorescence properties of deglycosylated milin were identical when excited at either 278 or 292 nm. Deglycosylated milin exhibited a fluorescence emission maximum at 340 nm instead of 333 nm for native glycosylated milin (Fig. 1b) (Yadav et al. 2009, 2010). Fluorescence intensity of deglycosylated milin was gradually increasing with chaotropes concentration at pH 7.0 while it

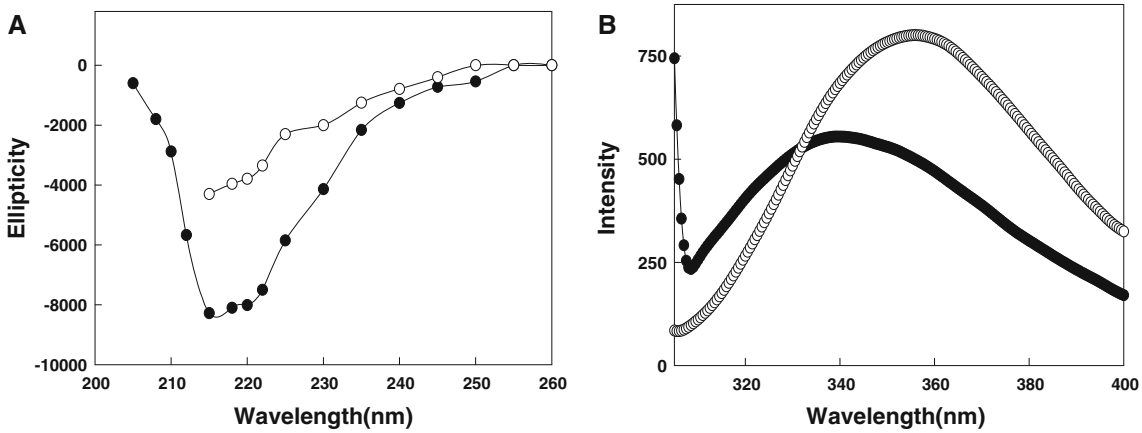

Fig. 1 Spectroscopic characterization of deglycosylated milin; milin was deglycosylated by TFMS and dissolved in 1.5 M GuHCl, taken as native deglycosylated milin. **a** Far-UV spectra of native (*filled circles*) and denatured (*open circles*) deglycosylated milin. Protein concentration for far-UV CD measurements was 0.1 mg/ml. **b** Intrinsic fluorescence spectra of native (*filled circles*) and denatured (*open circles*) deglycosylated milin. Protein concentration was 0.01 mg/ml for fluorescence measurements. Samples were incubated under given conditions for 24 h at room temperature before measurements

was decreasing at pH 2.0. Deglycosylated milin retained its native-like fluorescence spectrum at pH 2.0, like glycosylated milin (Yadav et al. 2010). The fluorescence emission maximum was red-shifted from 340 to 358 nm and fluorescence intensities increased by up to 50–60% on complete unfolding of deglycosylated milin by GuHCl and urea at neutral pH.

ANS binding

Exposure of hydrophobic surfaces of the enzyme was measured by its ability to bind to the fluorescent dye ANS. ANS binded strongly to deglycosylated milin compared with native glycosylated milin (Yadav et al. 2010). A blue-shift of 40 nm of the ANS emission maximum (from 520 to 480 nm) was observed in comparison with ANS spectra for native and denatured deglycosylated milin (Fig. 2). ANS binding was not observed for the intermediary concentration of chaotropes or after complete unfolding of deglycosylated milin.

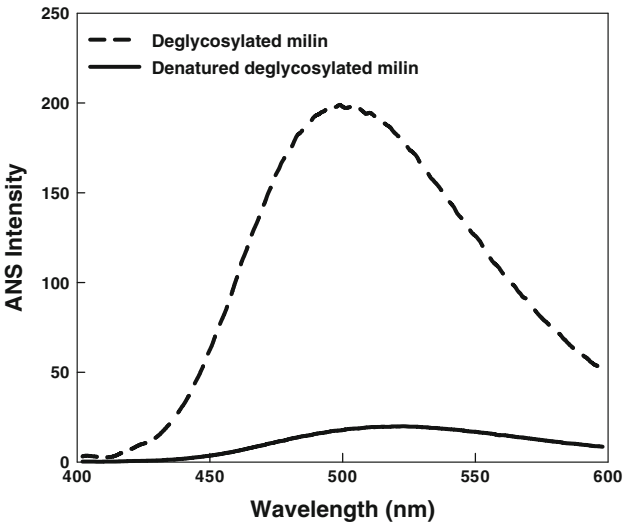

Fig. 2 ANS binding to deglycosylated milin. ANS binds strongly to deglycosylated milin (*dash line*) in comparison with denatured deglycosylated (*solid line*) milin. Protein concentration used was 0.015 mg/ml. Deglycosylated milin was incubated in the dark with 100-fold molar excess of ANS for more than 30 min at room temperature, and ANS fluorescence was measured at 400–600 nm on excitation at 380 nm. Conditions are indicated in the figure

Urea-induced denaturation of deglycosylated milin

Glycosylated milin was stable in 8 M urea from pH 7.0 to pH 2.0 so that complete transitions could not be obtained (Yadav and Jagannadham 2009; Yadav et al. 2009, 2010). However, deglycosylated milin was completely unfolded by urea at neutral pH. Urea-induced unfolding revealed stable inactive intermediate at neutral pH. This intermediate was stable from 5.5 to 6.5 M total chaotropes concentration (including 1.5 M GuHCl for solubility) at pH 7.0. The mean residual ellipticity, $[\theta]_{MRW}$, of intermediate was $-4{,}800$ deg cm^2/dmol. This intermediate appeared at the same chaotropes concentration when monitored by various probes, although the transition curves were not coincidental (Fig. 3a). Far-UV CD and fluorescence wavelength maxima were noncoincidental but similar in nature (Fig. 3a). The first transition midpoint (Cm_1) was at 5.0 M; however, the second transition midpoint (Cm_2) was at 7.5 M total chaotropic concentration (urea + 1.5 GuHCl). The urea-induced transition of deglycosylated milin was noncooperative, biphasic, and noncoincidental at pH 7.0. Unfolding of deglycosylated milin in the presence of urea at pH 2.0 followed a similar pattern but unfolding started at lower urea concentration (Fig. 3b). The intermediates in acidic

conditions were stable in 5.0–6.0 M urea including 1.5 M GuHCl, and the transition midpoints (C_{m1} and C_{m2}) were 4.5 and 7.0 M total chaotropes, respectively. The fluorescence intensity was gradually increasing (up to 50–60%) at neutral pH and decreasing (up to 40–50%) with acidic pH (Fig. 3a, b inset). Denaturation curves in acidic and neutral condition were noncoincidental as shown by far-UV CD, fluorescence intensity, and intrinsic fluorescence wavelength maxima (Fig. 3).

GuHCl denaturation of deglycosylated milin

GuHCl-induced unfolding of deglycosylated milin at neutral and acidic pH was measured by changes in far-UV CD, UV absorbance, and fluorescence. GuHCl-induced unfolding at pH 7.0 was broad (3.0–6.0 M), cooperative, and noncoincidental (Fig. 4a). The broad unfolding transition at pH 7.0 reveals the possibility of involvement of undetectable intermediates. However, the GuHCl transition at pH 2.0 was coincidental and cooperative (Fig. 4b). The combined effect of acid and GuHCl acted as a strong denaturizing agent, and thus the unfolding transition was sharp, cooperative, and coincidental without involvement of intermediates. Complete loss of secondary structure and a red-shift of the emission maxima from 340 to 358 nm were evident at both pH values in GuHCl-induced denaturation. The increasing and decreasing patterns of fluorescence intensity were similar to those for urea-induced unfolding.

Discussion

TFMS effectively cleaves *N*- and *O*-linked glycans nonselectively without affecting the functional structure of glycoproteins (Edge 2003). This makes TFMS an excellent deglycosylation agent for proteins in folded form, unlike enzymatic deglycosylation. Enzymatic deglycosylation (e.g., using PNGase F) requires completely unfolded protein to deglycosylate the glycoprotein. TFMS deglycosylation of milin in the presence of the scavenger yielded highly structured and folded deglycosylated milin. Anisole was found to be a suitable scavenger to neutralize the reactive group formed during the TFMS deglycosylation reaction. This has a positive impact in protecting the structural organization of milin due to neutralization of the extremely acidic nature of TFMS (data not shown). Compared with other scavengers (toluene, etc.), anisole yielded the most structured deglycosylated milin with similar molar ellipticity to that of glycosylated milin. The loss of solubility of milin on deglycosylation may be due to disturbance of the ionic balance. We have applied several conditions (data not shown) to solubilize the deglycosylated milin, but it was found to be soluble in 1.5 M GuHCl at neutral pH (Edge 2003). The kinetic stability of milin is completely lost and the protein does not show different mobility in heating and nonheating condition on SDS–PAGE, like glycosylated milin (data not shown) (Yadav et al. 2009). This confirms the crucial role of glycosylation in maintaining the kinetic stability of milin. Glycosylation in milin may be responsible for the dimerization, because deglycosylation leads to monomeric milin (Yadav et al. 2009). The kinetic stability and dimerization of protein are strongly correlated (Xia et al. 2007). Thus, the loss of these properties of deglycosylated milin confirms that glycosylation may be critical to maintain solubility, kinetic stability, and dimeric association. This behavior of milin is similar to that of human formyl peptide receptor (FPR) (Cupo et al. 1989; Malech et al. 1985; Quehenberger et al.

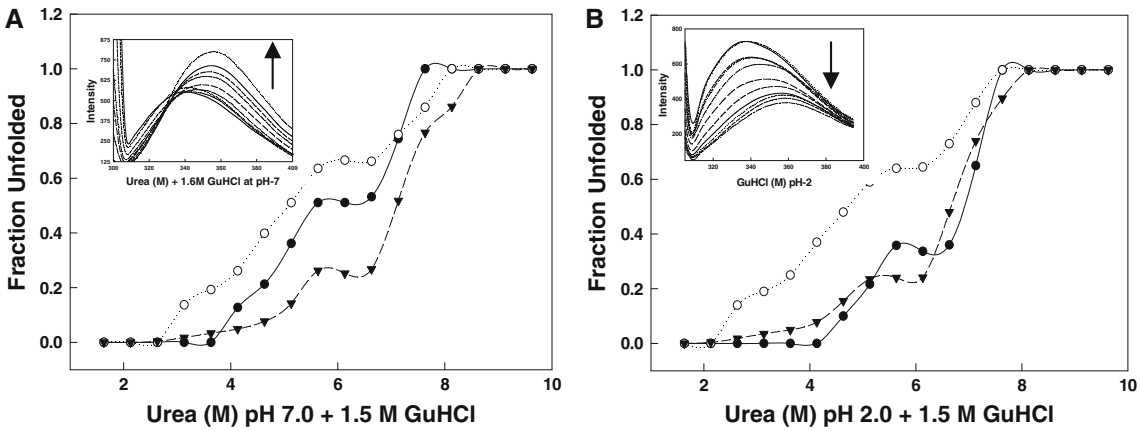

Fig. 3 Urea-induced unfolding of deglycosylated milin; the urea transition was monitored at different molarity of urea at **a** pH 7.0 and **b** pH 2.0. The unfolding transition shows far-UV CD ellipticity at 215 nm (*filled circle*), fluorescence wavelength maxima (*open circle*), and fluorescence intensity (*filled inverted triangles*) at increasing urea concentration. The *arrow* indicates the increase (*up arrow*) or decrease (*down arrow*) of fluorescence intensity upon increasing the concentration of chaotropes. The *inset* shows complete fluorescence spectra at each urea concentration

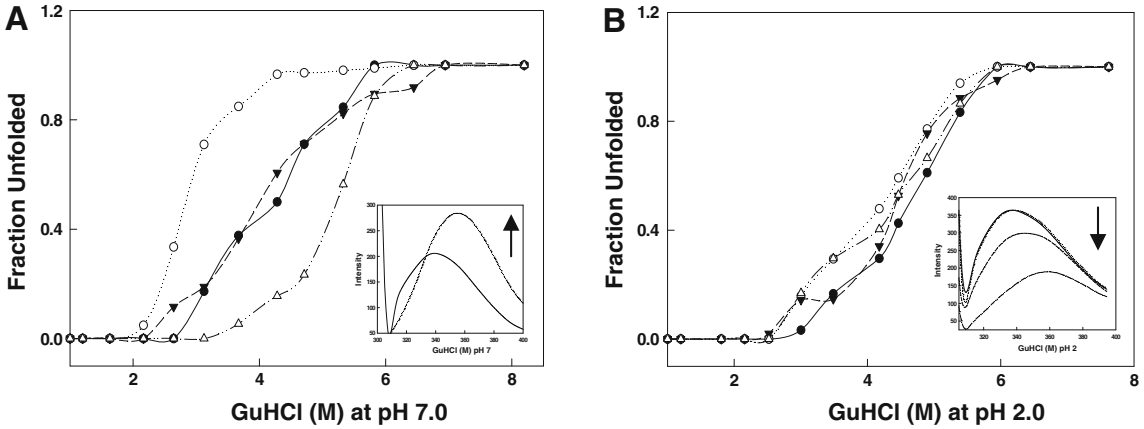

Fig. 4 GuHCl-induced unfolding of deglycosylated milin; the GuHCl transition was monitored at different molarities of GuHCl at **a** pH 7.0 and **b** pH 2.0. The unfolding transition shows far-UV CD ellipticity at 215 nm (*filled circles*), absorbance at 280 nm (*open circles*), and fluorescence wavelength maxima (*inverted filled triangles*) and fluorescence intensity (*open triangles*) at increasing concentration of GuHCl. The *inset* shows the fluorescence spectra at some concentration of GuHCl and the *arrow* indicates the increase (*up arrow*) or decrease (*down arrow*) of fluorescence intensity upon increasing the concentration of chaotropes. At neutral pH the curves are noncoincidental, but at pH 2.0 they are coincidental

1992; Wenzel-Seifert et al. 1998). Differentially glycosylated subunits such as those in milin are also reported in catalytic chains of RgpB enzymes. This protein is differentially modified by the posttranslational addition of different carbohydrate moieties. Glycosylation of milin provides extra stability of dimeric subunit association and may not facilitate dimerization. Acidic pH (>2), 2–3 M GuHCl, and 4–5 M urea induce molten globule state in native milin (Yadav et al. 2010). The presence of 1.5 M GuHCl is responsible for the formation of the molten globule state in deglycosylated milin, because native milin behaves as a molten globule state at this chaotrope concentration. This indicates that these protease isoforms are modified not only to a different extent but also with different sugars moieties (Curtis et al. 1999).

Deglycosylation of milin leads to reduction in α-helicity (20%) (Fig. 1a). However, glycosylated and deglycosylated milin have similar far-UV CD spectrum in 1.5 M GuHCl (Yadav et al. 2010). This is an indication of preservation of complete secondary structure of milin after deglycosylation. The loss of proteolytic activity may be due to change in functional attribute and exposure to strong acidic condition during TFMS deglycosylation. This acidic exposure may create exposed hydrophobic patches that bind with ANS, similar to in native glycosylated milin (Fig. 2) (Yadav et al. 2009). Another possible explanation for this loss of activity may be involvement of glycosylation in the regulation or protection of activity, as reported for GPCRs (Wenzel-Seifert and Seifert 2003). The reduction in α-helical content after deglycosylation of milin is similar to the case of recombinant apoLp-III. Recombinant apoLp-III has lower α-helical content than does glycosylated apoLp-III (Soulages et al. 1998). The results suggest that the loss of activity after deglycosylation is due to exposure of hydrophobic domains and/or alteration of the conformational flexibility of the protein (Soulages et al. 1998). This finding indicates that glycosylation plays an important role in normal function and maintenance of proteolytic action of milin like in FPR (Wenzel-Seifert and Seifert 2003).

Quantum yields of fluorescence are decreased due to interaction of chromophores with quenching agents either in the solvent or the protein itself. The final 18 nm red-shift (after unfolding) in the fluorescence wavelength maximum from 340 to 358 nm is due to exposure of tryptophan residues to a polar environment. The decrease in fluorescence intensities may be due to a decrease in distance between tryptophan and specific quenching groups, such as protonated carboxyl, protonated imidazole, deprotonated amino groups, and tyrosinate (Halfman and Nishida 1971). The decrease (at acidic pH) or increase (at neutral pH) in intensity is probably due to the effect of pH and is not dependent upon the denaturant for deglycosylated milin (inset of Figs. 2, 3). However, the similar fluorescence intensity at pH 7.0 and pH 2.0 indicates high intramolecular quenching between the chromophores and quenchers (data not shown).

The rate of unfolding of deglycosylated milin is higher than for glycosylated milin. This is because the rate of unfolding is inversely proportional to the amount of glycosylation, even though the folding mechanism is highly conserved (Grafl et al. 1987). Urea induces complete unfolding of deglycosylated milin, unlike for native milin (Yadav and Jagannadham 2009; Yadav et al. 2010). Urea-induced transition at neutral pH revealed a stable intermediate [$I_{(deg)N}$] in 4–5 M urea (excluding 1.5 M GuHCl).

A similar intermediate [$I_{(deg)A}$] was observed in 3.5–4.5 M urea at acidic pH 2.0. Neither of these intermediates bind to ANS. The fluorescence wavelength maxima shifted to 346–348 nm compared with 340 nm for native deglycosylated milin (Fig. 5). Complete unfolding occurred at 8.5 and 7.5 M chaotropes at pH 7.0 and at pH 2.0, respectively (Fig. 3). The total chaotropes concentration represented in the folding scheme and figures are the sum of urea concentration plus 1.5 M GuHCl. The noncoincidental and noncooperative transitions of milin may provide an indication of the sequential unraveling of different layers of monomeric α/β protein (Yadav et al. 2009). Completely unfolded milin is observed at 6 M GuHCl at pH 7.0 and 2.0 without the involvement of any detectable unfolding intermediates. This confirms the reduction in stability of deglycosylated milin in comparison with glycosylated milin. It is noted that the native proteins are stable in 6 M GuHCl at neutral pH; however, deglycosylated milin shows complete unfolding (Yadav et al. 2010). Thus, it is clear that deglycosylated milin attains a monomeric state and undergoes unfolding via monomeric inactive intermediates (Yadav et al. 2009), similar to dimeric protein desulfoferrodoxin (Apiyo et al. 2001).

The folding scheme explains the complexity of the protein unfolding mechanism (Fig. 5). The protein followed the unfolding route $\mathbf{N_2} \rightarrow \mathbf{I_{deg}} \rightarrow \mathbf{I_{(deg)N}}$ or $\mathbf{I_{(deg)A}} \rightarrow \mathbf{U}$ (**I** designates intermediate, subscript $_{(2)}$ designates dimeric state, $_{(deg)}$ for deglycosylated milin, **U** for unfolded protein, and subscript $_{(N)}$ and $_{(A)}$ for neutral and acidic condition, respectively). The $\mathbf{N_2} \rightarrow \mathbf{I_{deg}}$ conversion is due to deglycosylation and after dissolution of milin in 1.5 M GuHCl. Two monomeric intermediates, $\mathbf{I_{(deg)N}}$ and $\mathbf{I_{(deg)A}}$, are involved in urea-induce unfolding (Fig. 5). The

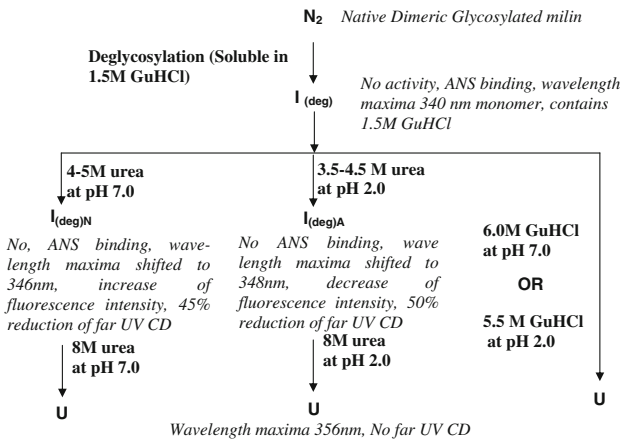

Fig. 5 Schematic representation of intermediate in unfolding of deglycosylated milin: the intermediate states along with their characteristics features. The naming of intermediates indicates: type of intermediate (monomeric **I**), deglycosylation ($_{deg}$), and condition ($_{(N)}$ for pH 7.0 and $_{(A)}$ for pH 2.0)

deglycosylated proteins strongly bind with ANS, thus accomplishing a molten-globule-like structure (Fig. 2). This molten globule structure directly forms the unfolded monomer without detectable intermediates on GuHCl transition at pH 7.0 and 2.0 (Fig. 4).

Conclusions

The dimeric association, structural stability, and solubility of milin were lost after deglycosylation. The presence of stable intermediates in the unfolding routes of milin is nature's way of keeping proteins stably folded, and avoiding undesirable unfolding events. These contacts as well as kinetic stability in milin may be provided by glycosylation. Finding means to enhance kinetic stability could be a viable and reasonable strategy for development of highly stable proteases. Investigation of deglycosylated milin provides a way to understand the mechanism of structural stabilization against denaturation.

Acknowledgments Financial assistance to S.C.Y. from the Council of Scientific and Industrial Research (CSIR) Government of India, in the form of a research fellowship and the financial assistance from UGC and DBT, Government of India, for infrastructure are acknowledged.

References

Apiyo D, Jones K, Guidry J, Wittung-Stafshede P (2001) Equilibrium unfolding of dimeric desulfoferrodoxin involves a monomeric intermediate: iron cofactors dissociate after polypeptide unfolding. Biochemistry 40:4940–4948

Bernard BA, Newton SA, Olden K (1983) Effect of size and location of the oligosaccharide chain on protease degradation of bovine pancreatic ribonuclease. J Biol Chem 258:12198–12202

Bosques CJ, Tschampel SM, Woods RJ, Imperiali B (2004) Effects of glycosylation on peptide conformation: a synergistic experimental and computational study. J Am Chem Soc 126:8421–8425

Cassim JY, Yang JT (1969) A computerized calibration of the circular dichrometer. Biochemistry 8:1947–1951

Cupo JF, Allen RA, Jesaitis AJ, Bokoch GM (1989) Reconstitution and characterization of the human neutrophil *N*-formyl peptide receptor and GTP binding proteins in phospholipid vesicles. Biochim Biophys Acta 982:31–40

Curtis MA, Thickett A, Slaney JM, Rangarajan M, Aduse-Opoku J, Shepherd P, Paramonov N, Hounsell EF (1999) Variable carbohydrate modifications to the catalytic chains of the RgpA and RgpB proteases of Porphyromonas gingivalis W50. Infect Immun 67:3816–3823

Daniels R, Kurowski B, Johnson AE, Hebert DN (2003) N-linked glycans direct the cotranslational folding pathway of influenza hemagglutinin. Mol Cell 11:79–90

Edge AS (2003) Deglycosylation of glycoproteins with trifluoromethanesulphonic acid: elucidation of molecular structure and function. Biochem J 376:339–350

Gagneux P, Varki A (1999) Evolutionary considerations in relating oligosaccharide diversity to biological function. Glycobiology 9:747–755

Grafl R, Lang K, Vogl H, Schmid FX (1987) The mechanism of folding of pancreatic ribonucleases is independent of the presence of covalently linked carbohydrate. J Biol Chem 262:10624–10629

Halfman CJ, Nishida T (1971) Nature of the alteration of the fluorescence spectrum of bovine serum albumin produced by the binding of dodecyl sulfate. Biochim Biophys Acta 243:294–303

Hirsch C, Misaghi S, Blom D, Pacold ME, Ploegh HL (2004) Yeast *N*-glycanase distinguishes between native and non-native glycoproteins. EMBO Rep 5:201–206

Imperiali B, O'Connor SE (1999) Effect of N-linked glycosylation on glycopeptide and glycoprotein structure. Curr Opin Chem Biol 3:643–649

Kuster B, Krogh TN, Mortz E, Harvey DJ (2001) Glycosylation analysis of gel-separated proteins. Proteomics 1:350–361

Lynn KR, Clevette-Radford NA (1988) Proteases of euphorbiaceae. Phytochemistry 27:45–50

Malech HL, Gardner JP, Heiman DF, Rosenzweig SA (1985) Asparagine-linked oligosaccharides on formyl peptide chemotactic receptors of human phagocytic cells. J Biol Chem 260:2509–2514

O'Conner SE, Imperiali B (1998) A molecular basis for glycosylation-induced conformational switching. Chem Biol 5:427–437

O'Connor SE, Imperiali B (1996) Modulation of protein structure and function by asparagine-linked glycosylation. Chem Biol 3:803–812

Pace CN, Shirley BA, McNutt M, Gajiwala K (1996) Forces contributing to the conformational stability of proteins. Faseb J 10:75–83

Petrescu SM, Branza-Nichita N, Negroiu G, Petrescu AJ, Dwek RA (2000) Tyrosinase and glycoprotein folding: roles of chaperones that recognize glycans. Biochemistry 39:5229–5237

Quehenberger O, Prossnitz ER, Cochrane CG, Ye RD (1992) Absence of G(i) proteins in the Sf9 insect cell. Characterization of the uncoupled recombinant *N*-formyl peptide receptor. J Biol Chem 267:19757–19760

Reuter G, Gabius HJ (1999) Eukaryotic glycosylation: whim of nature or multipurpose tool? Cell Mol Life Sci 55:368–422

Shental-Bechor D, Levy Y (2008) Effect of glycosylation on protein folding: a close look at thermodynamic stabilization. Proc Natl Acad Sci U S A 105:8256–8261

Soulages JL, Pennington J, Bendavid O, Wells MA (1998) Role of glycosylation in the lipid-binding activity of the exchangeable apolipoprotein, apolipophorin-III. Biochem Biophys Res Commun 243:372–376

Stryer L (1965) The interaction of a naphthalene dye with apomyoglobin and apohemoglobin. A fluorescent probe of non-polar binding sites. J Mol Biol 13:482–495

Varki A (1993) Biological roles of oligosaccharides: all of the theories are correct. Glycobiology 3:97–130

Wenzel-Seifert K, Seifert R (2003) Critical role of N-terminal N-glycosylation for proper folding of the human formyl peptide receptor. Biochem Biophys Res Commun 301:693–698

Wenzel-Seifert K, Hurt CM, Seifert R (1998) High constitutive activity of the human formyl peptide receptor. J Biol Chem 273:24181–24189

Wujek P, Kida E, Walus M, Wisniewski KE, Golabek AA (2004) N-glycosylation is crucial for folding, trafficking, and stability of human tripeptidyl-peptidase I. J Biol Chem 279:12827–12839

Xia K, Manning M, Hesham H, Lin Q, Bystroff C, Colon W (2007) Identifying the subproteome of kinetically stable proteins via diagonal 2D SDS/PAGE. Proc Natl Acad Sci U S A 104:17329–17334

Yadav SC, Jagannadham MV (2009) Complete conformational stability of kinetically stable dimeric serine protease milin against pH, temperature, urea, and proteolysis. Eur Biophys J 39:981–991

Yadav SC, Pande M, Jagannadham MV (2006) Highly stable glycosylated serine protease from the medicinal plant Euphorbia milii. Phytochemistry 67:1414–1426

Yadav SC, Jagannadham MV, Kundu S (2009) A kinetically stable plant subtilase with unique peptide mass fingerprints and dimerization properties. Biophys Chem 139:13–23

Yadav SC, Kundu S, Jaganadham MV (2010) Equilibrium unfolding of kinetically stable serine protease milin: presence of various active and inactive dimeric intermediates. Eur Biophys J (in press)